





# Enhanced cytotoxicity of docetaxel delivered through folic acid grafted poloxamer P188 polymeric micelles

Amol TATODE <sup>1</sup> , Divya ZAMBRE <sup>1</sup> , Mohammad QUTUB <sup>1\*</sup> , Tanvi PREMCHANDANI <sup>1</sup> ,  
Milind UMEKAR <sup>1</sup> , Prashant PANDE <sup>2</sup> 

<sup>1</sup> Department of Pharmaceutics, Smt. Kishoritai Bhoyar College of Pharmacy, Kamptee, Nagpur, Maharashtra, 441002 India.

<sup>2</sup> Department of Civil Engineering, Yeshwantrao Chavan College of Engineering, Nagpur, Maharashtra, 441110 India.

\* Corresponding Author. E-mail: qutubmalikqm@gmail.com (M.Q.); Tel. +91-997-046 18 94.

Received: 16 August 2024 / Revised: 23 September 2024 / Accepted: 26 September 2024

**ABSTRACT:** Nanotechnology-based drug delivery systems have gained significant attention for improving cancer treatment. In this study, folic acid (FA)-conjugated Poloxamer P188 (FA-P188) micelles were developed for targeted delivery of docetaxel (DTX) to cancer cells that overexpress folate receptors. The micelles were prepared using the thin-film hydration method, where polymers and DTX were dissolved in an organic solvent, followed by solvent evaporation to form a thin film, which was then hydrated with water to form micelles. The critical micelle concentration (CMC) was determined using UV spectroscopy with an iodine standard solution. Micelle size, polydispersity index (PDI), and surface charge were characterized using dynamic light scattering, and the morphology was visualized through scanning electron microscopy. Entrapment efficiency of DTX in micelles was quantified using ultracentrifugation and UV spectrophotometry, after separating the unencapsulated drug. In vitro drug release kinetics were assessed via dialysis and UV spectroscopy. Hemocompatibility was tested by measuring hemoglobin release from red blood cells using spectrophotometry. The anticancer efficacy of the DTX formulations was evaluated in MDA-MB-231 breast cancer cells using the MTT assay after a 72-hour exposure. Stability of the FA-P188-DTX micelles was assessed under accelerated conditions (40°C, 75% relative humidity) for three months. The study's findings showed successful conjugation of FA to P188 and effective encapsulation of DTX in FA-P188 micelles. The optimized FA-P188-DTX micelles demonstrated particle sizes smaller than 200 nm, a PDI of less than 0.2, and a drug entrapment efficiency exceeding 75%. In vitro cytotoxicity assays showed enhanced cytotoxicity of FA-P188-DTX micelles in MDA-MB-231 cancer cells compared to DTX alone and non-targeted micelles. These results highlight the targeting capability and sustained drug release properties of FA-P188-DTX micelles, suggesting their promising potential for targeted cancer therapy involving docetaxel.

**KEYWORDS:** Docetaxel; targeted drug delivery; polymeric micelles; folic acid; cancer therapy.

## 1. INTRODUCTION

Despite considerable advances in anticancer therapy, cancer disease remains one of the world's primary health issues. It remains a severe concern, even though significant efforts have been taken over the last several decades, as indicated by numerous clinical interventions and anticancer therapeutics [1]. Chemotherapy is a common treatment that uses drugs or a combination of drugs to kill rapidly developing cancer cells [2]. Instead of damaging normal cells, the drugs must target tumor cells. Chemotherapeutic agents are highly toxic and have limited clinical applicability, which limits their use alone. Among the various recently developed cancer therapies, targeted cancer therapy is gradually replacing chemotherapy and becoming a prominent treatment option for human cancers [3,4]. Recently, Nanoparticle-based drug delivery systems have gained increasing attention in cancer therapy because of their benefits which include tumor cell targeting, reduced side effects, and drug resistance; and are constructed based on tumor pathophysiology [5–7]. It is difficult to find a mechanism for the effective delivery of anti-cancer drugs because most of them are hydrophobic.

**How to cite this article:** Tatode A, Zambre D, Qutub M, Premchandani T, Umekar M, Pande P. Enhanced cytotoxicity of docetaxel delivered through folic acid grafted poloxamer P188 polymeric micelles. J Res Pharm. 2025; 29(5): 2126-2142.

As nanocarriers, polymeric micelles are becoming much more popular [8–10]; because of their unique core-shell structure which can physically embed or chemically link the hydrophobic drug into the hydrophobic core, increasing the drug's water solubility [11,12]. Furthermore, micelles have various distinct advantages, including drug accumulation in tumor sites due to the EPR effect, sustained drug release behavior, and extended drug circulation time due to the lack of rapid renal clearance [13,14]. To develop a more effective site-specific drug delivery system, targeted ligands can be bound to the surface of the micelle [15]. Cancer cells have highly expressed folate receptors on their surfaces, even if normal cells have folate receptors, they are at low or undetectable levels [16,17]. Folic acid (FA) as a targeting agent, due to its high binding affinity to folate receptors, has shown a promising future in targeted drug delivery systems [18–20]; therefore it can be introduced to improve treatment efficiency while also avoiding toxic effects to normal cells. FA also keeps its high binding affinity to folate receptors after coupling with drug carriers [18,21]. Folate coupling serves several purposes, including delivering nonspecific drugs to cancer cells selectively, decreasing harmful side effects in healthy cells, and accelerating cell internalization via receptor-mediated endocytosis [22]. Amphiphilic block copolymers are used in nanomedicine because they have appealing features for tackling drug delivery challenges and have intrinsic biological activity [23]. Poloxamers belong to the amphiphilic triblock copolymer family [24,25]. It is composed of hydrophilic polyethylene oxide and hydrophobic polypropylene oxide blocks, and has an A-B-A triple block structure (PEO-PPO-PEO), which allows it to self-assemble into micelles in an aqueous environment [26]. Poloxamers are being used to make hydrophobic drugs soluble [27]. The use of Poloxamer to create unique potential nanomedicine has been well-documented for several years [24]. The hydrophobic PPO section serves as a hydrophobic core for integrating hydrophobic drugs, whereas the hydrophilic PEO aids in the prevention of aggregation [28,29]. They can improve solubility, circulation time, and drug release in target areas [30]. In this study, a tumor-targeting micellar system based on folate conjugated Poloxamer was designed for DTX delivery. The hydrophobic drug, DTX, was encapsulated in hydrophobic polypropylene oxide blocks of Poloxamer conjugated with folic acid to increase its solubility [31,32]. Developed through targeting using folate receptors, FA- P188 micelles containing DTX can improve the accuracy of drug delivery, increasing efficacy against cancer cells and reducing damage to normal cells.

## 2. RESULT AND DISCUSSION

### 2.1 Interaction studies of excipients

The study of interactions between adjuvants and drugs is an essential step in pre-formulation studies. DSC is an analytical method frequently used to assess drug-adjuvant interactions. Changes in endothermic or exothermic peaks and/or enthalpy values indicate possible interactions [33]. The DSC curves of the drug and drug-adjuvant mixture are shown in figure 1. The thermal behavior of pure drugs, corresponding adjuvants, and combinations of drugs and supplements will be compared on the DSC curve. DSC temperature grams of pure DTX showed a sharp endothermic peak at  $\sim 169^{\circ}\text{C}$ , which corresponds to the melting point. Poloxamer F 68 and Folsan exhibited rapid endothermic peaks at  $\sim 54^{\circ}\text{C}$  and  $\sim 140^{\circ}\text{C}$ , respectively. The temperature gram of the physical mixture (DTX: Poloxamer P188: folic acid) showed a slight and insignificant change in the thermal behavior of DTX in the presence of Poloxamer P188. The melting signal (endotherm) of Poloxamer P188 was distinguishable from the physical mixture of each polymer with DTX. The absence of other endothermic/exothermic events across the entire temperature range thus ruled out any physical interactions or compatibility between the drug and the polymer. Therefore, the DSC results indicated that these polymers are suitable for use in the formulations.

FTIR was performed to confirm the compatibility of individual components (Figure 2). The IR spectrum of Poloxamer P188- folic acid mixture was compared with the IR spectra of folic acid. FTIR of folic acid showed a characteristic peak at  $1605\text{cm}^{-1}$ ,  $1693\text{cm}^{-1}$  and  $1483\text{cm}^{-1}$  attributed to NH bending vibration of CONH, C=O amide stretching of a carbonyl group, and phenyl ring respectively and FTIR of P188 showed  $2883\text{cm}^{-1}$  and  $1342\text{cm}^{-1}$  attributed to CH stretching and OH bending respectively. The IR spectrum of the physical mixture showed characteristic peaks at  $1147\text{cm}^{-1}$ ,  $1714\text{cm}^{-1}$ ,  $2880\text{cm}^{-1}$ , and  $3482\text{cm}^{-1}$  attributed to NH, C=O, CH, and OH stretching respectively. The results confirmed the absence of any chemical interaction between folic acid and Poloxamer P188.

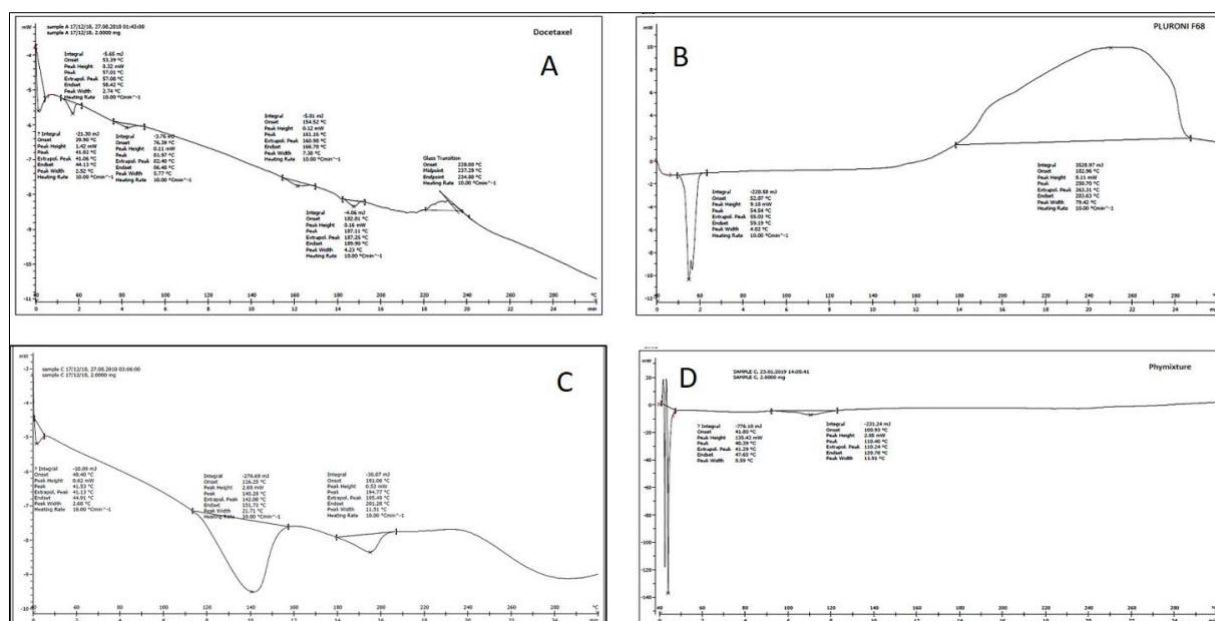


**Figure 1.** DSC Thermogram of A-Docetaxel, B- Poloxamer P188, C- Folic Acid, and D- Physical mixture

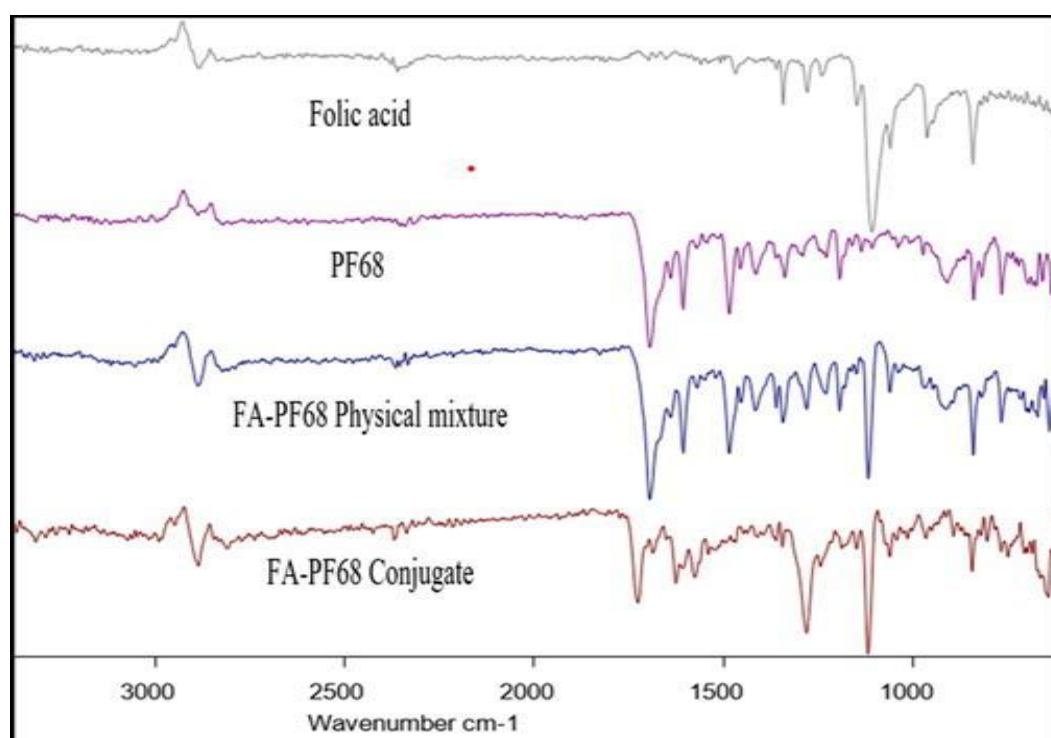


**Figure 2.** FT-IR of folic acid, Poloxamer P188, physical mixture, and FA-P188 conjugate

## 2.2 Characterization of FA-P188 conjugate

Figure 2 demonstrates the successful chemical bonding of FA-P188 with a characteristic peak of 1725 cm<sup>-1</sup> of the ester bond. Other characteristics of Folsan's carboxylate base IR absorption peaks have moved from 1690 cm<sup>-1</sup> to 1685 cm<sup>-1</sup>. As FTIR techniques alone are insufficient to confirm binding, <sup>1</sup>H NMR spectroscopy was also performed.

The NMR spectra of FA-P188 hydroxide (Figure 3) showed a broad peak (by PEO) at 3.5 ppm in DMSO-d<sub>6</sub>, and the FA signal was at 6.6 and 7.6 ppm (aromatic proton) and 8.6 ppm (phtheridine proton), confirming the success of the binding.

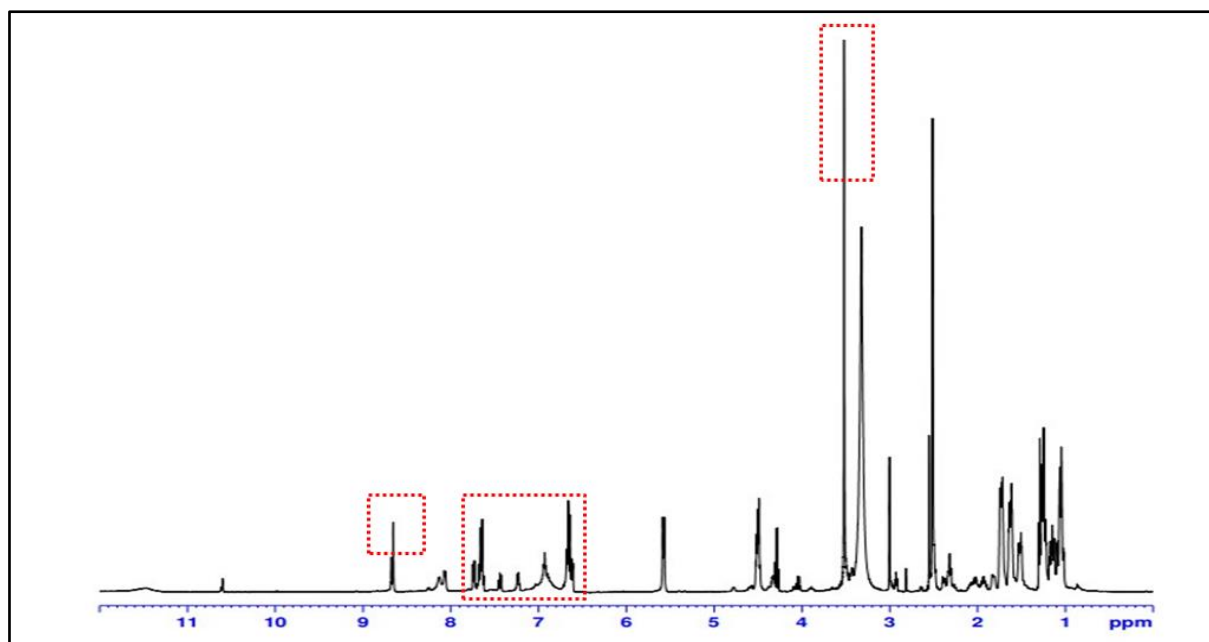


**Figure 3.**  $^1\text{H}$  NMR Spectrum of FA-P188 Conjugate in DMSO- $d_6$ , showing a characteristic peak at 3.5 ppm, 6.6-7.6, and 8.6 attributed to PEO, FA signals, and pteridine proton 6.6 and 7.6 ppm (aromatic proton) and 8.6 ppm (phtheridine proton), confirming the success of the binding [34].

### 2.3 Analysis of data and optimization of design

Using Design Expert DX 10.0.7.0 (Stat-Ease Inc., MN.), the results were statistically analyzed for the response variables. The  $3^2$ -factor design proposed nine formulations varying at three distinct levels (high, medium, and low) for two independent variables: the amount of binding polymer (FA-P188) and the amount of drug (DTX). In this study, the effects of these independent variables on carrier efficiency and particle size were investigated as optimization response variables. Table 1 illustrates the various experimental trials and the observed responses.

**Table 1.** Full factorial design ( $3^2$ ) experimental trial batches, with responses.

Formulation code	Factors		Responses	
	FA-P188 mg ( $X_1$ )	DTX mg ( $X_2$ )	% EE (%) ( $Y_1$ )	PS (nm) ( $Y_2$ )
F1	100	5	87.91	147
F2	100	10	81.32	150
F3	100	15	82.93	161
F4	150	5	90.25	142
F5	150	10	88.91	140
F6	150	15	83.32	148
F7	200	5	91.74	152
F8	200	10	89.78	156
F9	200	15	84.97	164

The software provided a suitable polynomial model equations that included the individual main effects and interaction effects [35]. The optimized model equations for  $Y_1$ (%EE) and  $Y_2$ (PS) as reactions are presented in the equations below.

$$Y_1 = 86.79 + 2.39X_1 - 3.11X_2$$

$$Y_2 = 140.89 + 2.33 X_1 + 5.33X_2 - 0.50X_1X_2 + 11.67X_1^2 + 3.67X_2^2$$

After taking into account the coefficients and the mathematical sign they have, conclusions were drawn using the fitted polynomial equation, a linear model for % EE, and a quadratic model for particle size.

The correlation coefficient ( $R^2$ ) of the linear model (0.8298) for response  $Y_1$  (% EE) and that of the quadratic model (0.9628) for response  $Y_2$  (PS) was found to be significant (Table 2). The coefficient of  $X_1$  was positive and that of  $X_2$  was negative in the equation for % entrapment efficiency, indicating that the dependent variable  $Y_1$  is directly proportional to  $X_1$  (amount of FA-P188) and inversely proportional to  $X_2$  (quantity of DTX). The coefficients for  $X_1$  and  $X_2$  are both positive in the equation for particle size, indicating that the dependent variable  $Y_2$  is directly proportional to  $X_1$  (quantity of FA-P188) and  $X_2$  (quantity of DTX), but the coefficient for  $X_1X_2$  is negative, indicating that the combined effect of the independent variables is inversely proportional to  $Y_2$ .

**Table 2.** Parameters of a selected model of responses.

Percent Entrapment Efficiency ( $Y_1$ )		Particle Size ( $Y_2$ )	
Selected model	Linear	Selected model	Quadratic
Std. dev.	1.78	Std. dev.	2.55
Mean	86.79	Mean	151.11
c. v. %	2.05	c. v. %	1.68
PRESS	39.18	PRESS	228.60
R-squared $R^2$	0.8298	R-squared $R^2$	0.9628
Adjusted $R^2$	0.7730	Adjusted $R^2$	0.9008
Predicted $R^2$	0.6481	Predicted $R^2$	0.5628
Adequate precision	10.723	Adequate precision	11.626

The results of ANOVA is presented in Table 3 showed that all models were significant ( $p < 0.05$ ) for all the response variables examined. The metanomial term ( $p > 0.05$ ) was removed from the polynomial equations to simplify the model.

**Table 3.** Analysis of variance table for dependent variables from full factorial design.

Source	df	Sum Square	Mean Square	F-value	p-value
<b>Percent Entrapment Efficiency (<math>Y_1</math>)</b>					
Model	2	92.38	46.19	14.62	<b>0.0049</b>
$X_1$	1	34.22	34.22	10.83	0.0166
$X_2$	1	58.16	58.16	18.41	0.0051
<b>Particle Size (<math>Y_2</math>)</b>					
Model	5	503.44	100.69	15.53	<b>0.0235</b>
$X_1$	1	32.67	32.67	5.04	0.1104
$X_2$	1	170.67	170.67	26.33	0.0143
$X_1X_2$	1	1.00	1.00	0.15	0.7207

Furthermore, Design-Expert software-generated three-dimensional response surface plots are depicted in Figure 4.

In a multicriteria decision strategy using numerical optimization techniques by probability functions and graphical optimization techniques by overlay plots, all responses with different objectives were optimized as illustrated in the figure. Dependent variable reactions and constraints on independent variables were used to produce an optimized formulation. These constraints were common to all formulations. Based on the plot above, the Design-Expert software determined the suggested concentration of the independent variable, with a maximum probability close to 1.0 [36]. The optimized batch selected using design expert software is given in Table 4.

### 3.4 Evaluation and validation of the optimized formulation

The statistically optimized formulation F4 met all the physicochemical criteria. The entrapment efficiency and particle size of the optimized formulation were calculated to confirm its theoretical prediction (Table 5). The observations of carrier efficiency percent (90.25%) and particle size (142 nm) were well matched with model predictions of carrier efficiency percent (90.29%) and particle size (140 nm). The relative error (%) between the predicted value and the experimental value was calculated for each response, and the value was found to be within  $\pm 2\%$ . The experimental data aligned with the projected values, affirming the reliability and accuracy of the model.



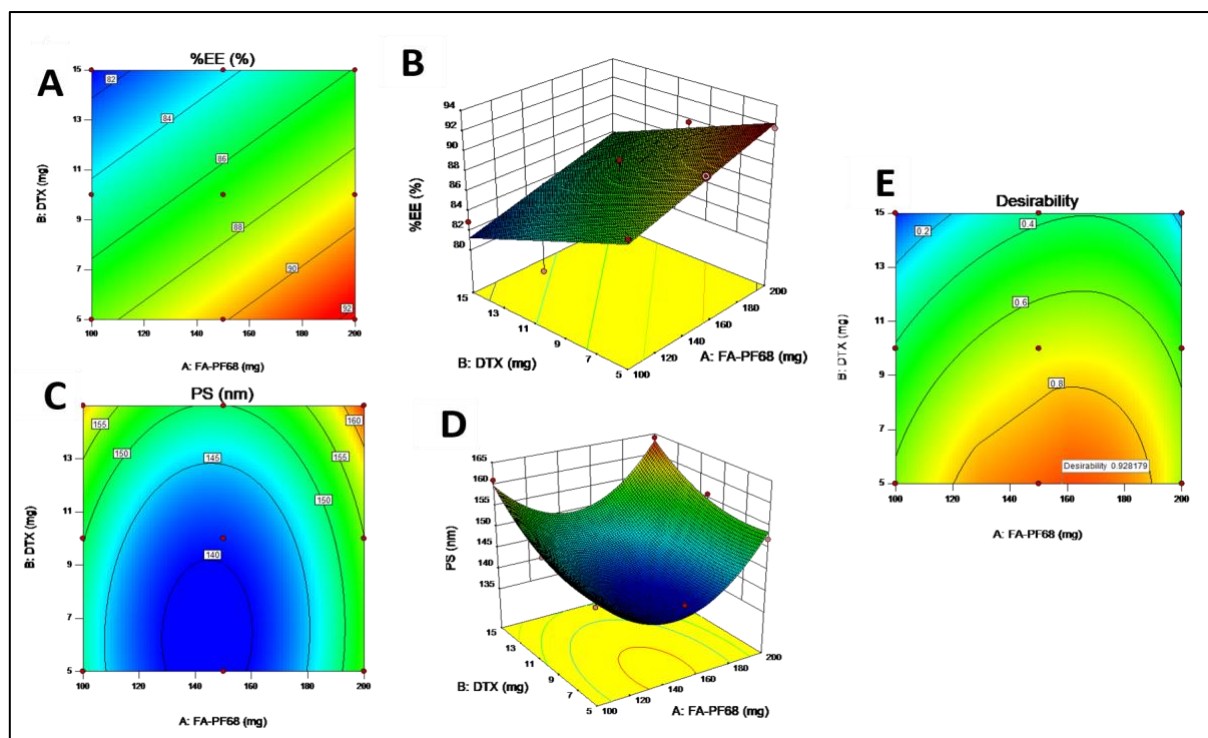


**Figure 4.** Contour plots and 3D response graphs of % entrapment efficiency (A & B), Particle size (C & D), and desirability plot of optimized batch (E).

**Table 4.** Characteristics of optimized batch.

Objects	FA-P188 (X <sub>1</sub> )	mg	DTX mg (X <sub>2</sub> )	Percent Entrapment Efficiency (Y <sub>1</sub> )	Particle Size (Y <sub>2</sub> )	Desirability	
Predicted	158		5	90.29	140	0.928	Selected
Actual (F4)	150		5	90.25	142		

**Table 5.** Validation of optimization model.

Response	Experimental Value	Predicted Value	% Relative Error
Percent Entrapment Efficiency (Y <sub>1</sub> )	90.25 %	90.29 %	-0.04 %
Particle Size (Y <sub>2</sub> )	142 nm	140 nm	-1.42 %

## 2.4 Characterization of P188-DTX & FA-P188-DTX Micelles

### 2.4.1 CMC Determination

CMC of the micelles have an impact on formulation's stability in both in vitro and in vivo conditions. CMC value was influenced by both the hydrophobic PPO length as well as the hydrophilic PEO length of Poloxamer P188. The CMC value was affected by the hydrophobic PPO length and the hydrophilic PEO length of the Poloxamer P188. In this study, iodine was used as a hydrophobic probe to observe the formation of micelles. The dissolved I<sub>2</sub> participates in the hydrophobic environment of the Poloxamer polymer and is converted to I<sup>2</sup> at I<sup>3-</sup> to maintain the saturated aqueous solution concentration of I<sup>2</sup>. I<sup>2</sup> absorbance was plotted for polymer concentration (Figure 5). It has been observed that the CMC of FA-P188 is lower than that of P188 [37].

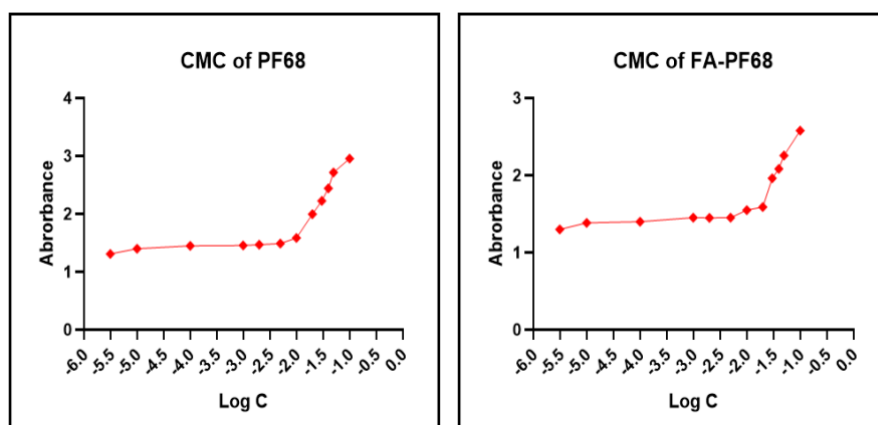


**Figure 5.** CMC determination of Poloxamer P188(P188) and folate conjugated Poloxamer P188 (FA-P188) by I<sub>2</sub> UV spectroscopy method.

## 2.4.2 Particle, polydispersity index, and zeta potential

The particle size of P188-DTX and FA-P188-DTX micelles was 152.2 nm at the highest % intensity of 79.1% and 142.2 nm with the highest % intensity of about 68.6 %. The P188-DTX and FA-P188-DTX micelles had polydisperse indices of 0.500 and 0.514, respectively (Figure 6).

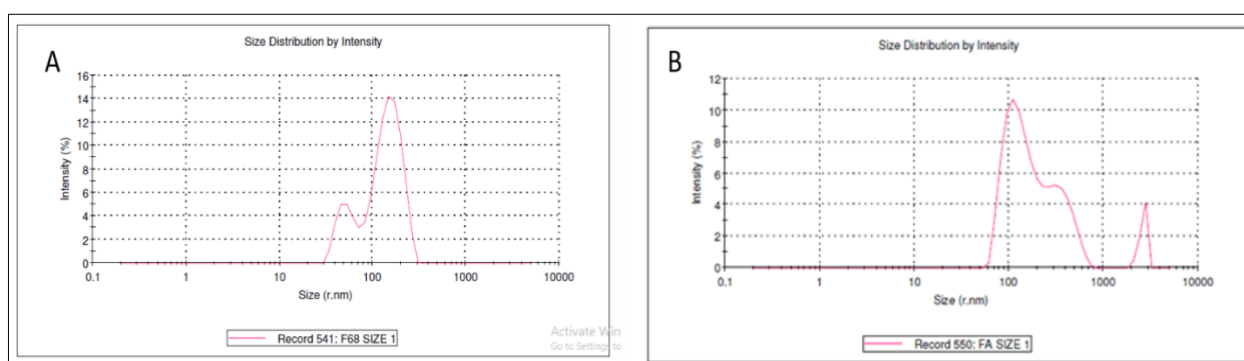


**Figure 6.** Particle size and distribution of A-P188-DTX Micelles and B-FA-PF8-DTX conjugated micelles.

Zeta potential is an important factor for assessing the stability of colloidal dispersions. The zeta potential value showed that the formulation had a negative charge, which indicates colloidal stability in aqueous solution. As depicted figure 7 zeta potential of the P188-DTX and FA-P188-DTX micelles was -14.4 mV and -15.8 mV, respectively.

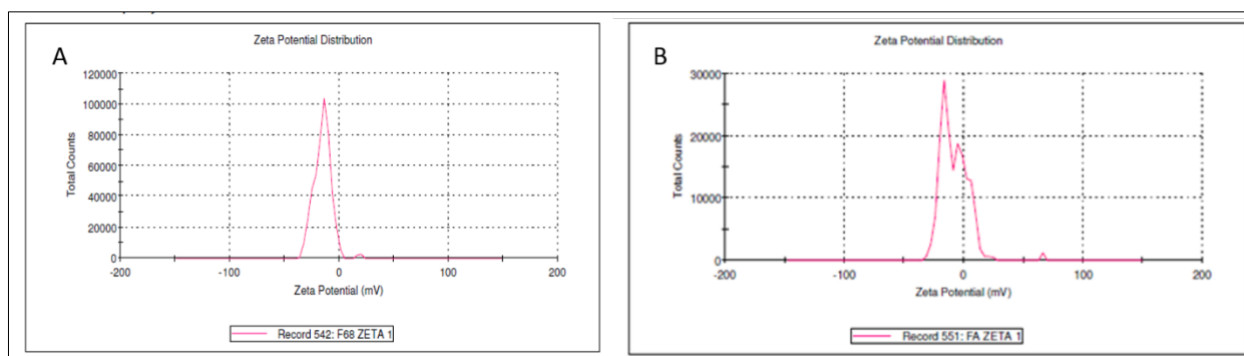


**Figure 7.** Zeta Potential of A-P188-DTX micelles and B-FA-PF8-DTX conjugated micelles.

### 2.4.3 Scanning electron microscopy (SEM)

The surface morphology of FA-P188-DTX conjugated micelles was analyzed by SEM at different magnifications 10000X and 3500X as shown in Figure 8. The micelles exhibit a shape close to spherical, and the drug was entrapped in the internal core of the micelles.

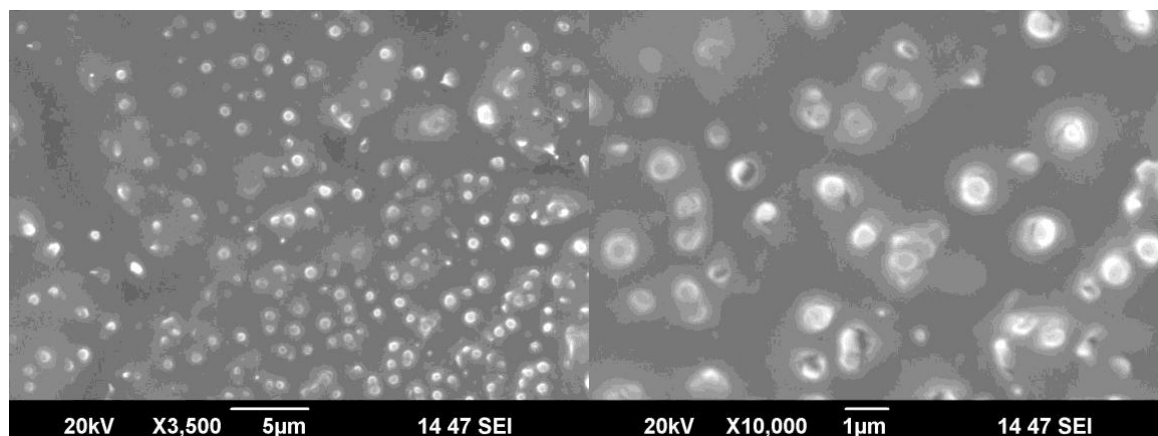


Figure 8. SEM Images of FA-PF8-DTX conjugated micelles

### 2.5 % Entrapment Efficiency

For drug delivery systems, drug encapsulation efficiency is essential. The entrapment efficiency of FA-P188-DTX micelles was found to be  $90.25 \pm 1.89\%$ .

### 2.6 In-vitro drug release

Using a dialysis tube, the release pattern of DTX from micelles was evaluated. The results demonstrate that FA-P188-DTX conjugated micelles released  $3.672 \pm 1.25\%$  of DTX within 1 hour. As seen in figure 9 during the first hour, the drug that was weakly bound or of micelles was released. FA-P188-DTX conjugated micelles displayed a pattern of sustained release that lasted for 24 hours. At the end of 24 hrs, the FA-P188-DTX-conjugated micelles released  $80.25 \pm 1.53\%$  of the DTX. The figure depicts the in vitro release of DTX, which reveals a sharp increase in DTX release at the 6th hour, which is due to the opening of pores in micelle walls. After the eighth hour, a constant release of DTX was noticed, which lasted for the next 24 hours. The tortuous type of diffusion release mechanism is confirmed by the release pattern of DTX in the surrounding aquatic environment. Furthermore, the drug release from P188-DTX micelles was investigated, and within 24 hours,  $47.56 \pm 0.89\%$  of DTX was released. It was witnessed that the amount of DTX released from folate-conjugated P188 micelles was approximately 30% more when compared with DTX released from P188 micelles [38].

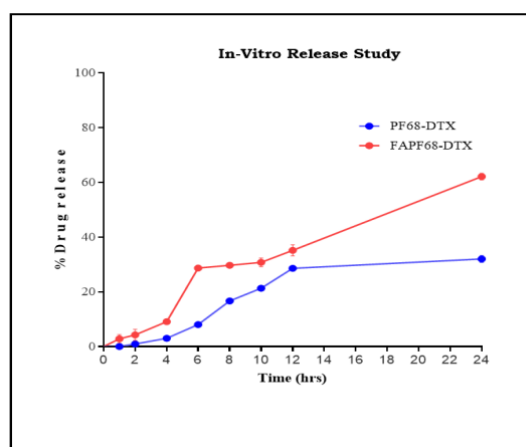
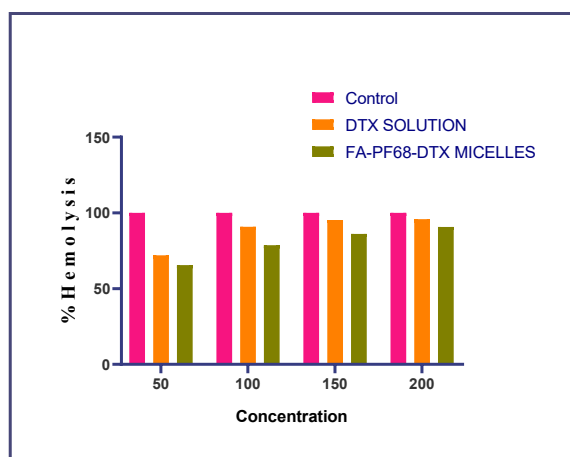


Figure 9. In-vitro release study of DTX from P188-DTX and FA-P188-DTX conjugated micelles.



## 2.7 Hemolytic toxicity studies

In this study, the docetaxel micellar formulation was compared with the docetaxel solution to evaluate hemolytic toxicity using an in vitro hemolysis assay. The hemolysis toxicity assay has been proposed as a toxicity test via in-vitro method as a simple and reliable measure for estimating the membrane damage that a formulation causes in in-vivo conditions. This assay quantitatively measures hemoglobin (Hb) release induced by formulation-red blood cell interactions. At 200 mg/mL concentration, a UV-visible spectrophotometer reading at 521 nm revealed a total of 73.18 percent hemolysis in FA-P188-DTX Micelles and 82.36% percent hemolysis DTX Solution. In this experiment, the amount of hemoglobin released by the interaction between the preparation and red blood cells was quantitatively measured, and the degree of hemolysis was quantified. In addition, qualitative information on morphological changes in red blood cells was obtained at the same time. According to the results, concentration-dependent hemolysis was observed in both preparations (Figure 10). The main reasons why micellar preparations showed lower hemolytic toxicity were the following two: First, DTX was encapsulated in surfactant, which limited its direct contact with erythrocyte cell membranes. Second, there was less cell membrane damage due to the absence of polysorbate and ethanol solvents. In other words, the introduction of the drug into the fast-contained core of the micelle reduced its direct contact with the erythrocyte cell membrane, thereby lowering hemolytic toxicity.



**Figure 10.** Hemolysis assay of FA-P188-DTX micelle formulation at various concentrations and its comparison with DTX solution.

Hemolytic toxicity of formulations was also assessed by optical microscopy and the effect of the interaction between the formulation and red blood cells on the shape of the red blood cells was visualized and photomicrographs are shown in figure 11. Morphologically intact red blood cells exhibit a typical disc shape similar to that of a bagel. During the hemolysis process, depending on the concentration of the hemolytic preparation and the degree of hemolysis, the shape of this disc changed to slightly drooping stomatocytes, like a goblet. In the event of complete hemolysis, a resemblance to cell fusion has been observed under the microscope.

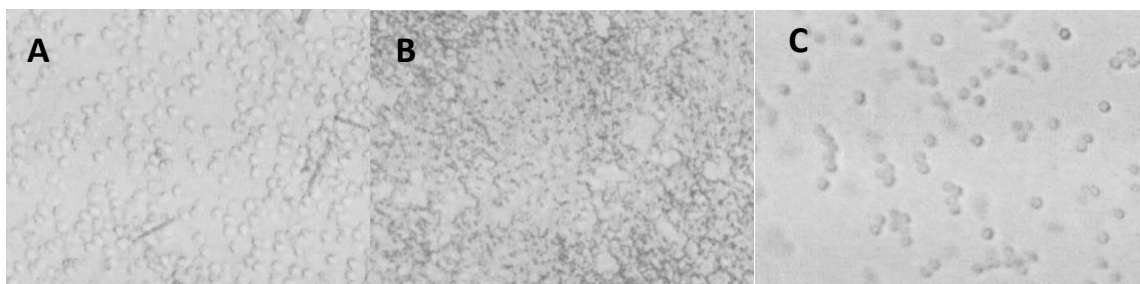


**Figure 11.** Photomicrographs of red blood cells incubate at 37°C for 1 h PBS 7.4 (A) saline solution (B), DTX solution (C), FA-P188-DTX micelles.

Photomicrographs showed very slight changes in the morphology of red blood cells treated with micellar preparations. On the other hand, when treated with DTX solution, almost complete hemolysis was observed. These results are well in line with the results of quantitative hemolytic toxicity tests.

## 2.8 Cytotoxicity studies

To investigate and validate the effectiveness and targeting capability of the prepared FA-P188-DTX micelles, MTT analysis was performed on the MDA-MB-231 human mammary adenocarcinoma cell line. The results showed that the percentage of cell survival of human mammary adenocarcinoma cells was significantly lower than that of DTX solution and blank micelles when compared to FA-P188-DTX micelles by concentration. This suggests that the formulation has increased cytotoxicity to cells (Figure 12).

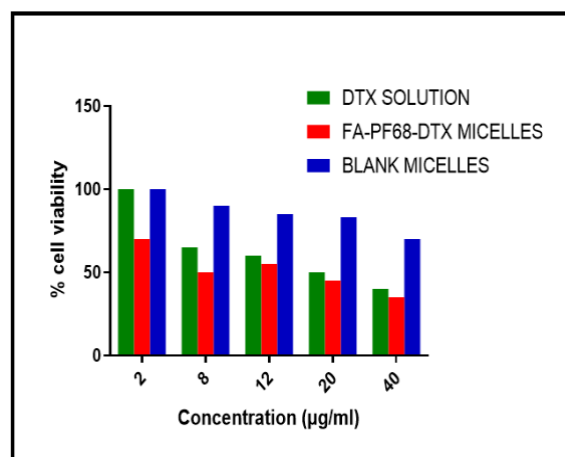


**Figure 12.** In vitro cell viability studies on MDA-MB-231 cell line by MTT Assay using DTX solution, FA-P188-DTX micelles and blank micelles.

## 2.9 Stability studies

As per ICH guidelines, the result of stability studies of FA-P188-DTX micelles formulation was evaluated for three months. FA-P188-DTX micelles did not show phase separation at 1 month and at the end of 3 months. Thus, the FA-P188-DTX micelles were seen to be stable after three months based on the findings of the stability research conducted under varied storage circumstances.

## 3. CONCLUSION

In this study, we developed a micelle-based drug delivery system consisting of a folate-bound P188 micelle loaded with a hydrophobic drug (DTX). Folic acid was conjugated with Poloxamer to target folate receptors which are overexpressed in the case of cancerous cells. The conjugate was synthesized by linking the hydroxyl group of P188 and the carboxyl group of folic acid by the esterification reaction. Using this conjugate FA-P188-DTX micelles were formed using the thin film hydration method. Response surface methodology i.e., 32 full factorial design has been successfully used for the optimization of the micelle formulation. The design proposed nine formulations for two independent variables: the quantity of conjugated polymer (FA-P188) and the drug (DTX), both of which were varied at three distinct levels (high, medium, and low) and their effect on independent variables, entrapment efficiency, and particle size was investigated. The cytotoxicity studies of DTX-loaded micelles showed improved anticancer effects against MDA-MB-231 cells in vitro due to enhanced active targeting via folic acid. Given that generating new drugs is a time-consuming and expensive procedure, thus enhancing the efficiency of existing drugs in various ways appears to be beneficial. Improving drug delivery strategies can decrease drug toxicity and increase effectiveness, favoring patient satisfaction and bringing pharmaceutical companies more benefits. Therefore, the FA-P188 bonded micelles loaded with DTX can be considered as a candidate with high potential for future use [39–41].

## 4. MATERIALS AND METHODS

### 4.1 Chemicals

Docetaxel was provided by Scino Pharmaceutical Pvt. Ltd., Taiwan; Poloxamer P188 was purchased from Loba Chemie Pvt. Ltd., Mumbai; Folic acid, Dimethylsulfoxide (DMSO), dimethylaminopyridine (DMAP) were obtained from Merck Specialities Pvt. Ltd., Mumbai; N N'-dicyclohexylcarbodiimide (DCC) was purchased from Himedia Laboratory Pvt. Ltd., Mumbai; Acetonitrile was obtained from Loba Chemie Pvt. Ltd., Mumbai; All other chemicals and solvents were of analytical or synthetic grade and were used without further purification. Distilled water was used in whole experimental procedures.

### 4.2 Interaction studies of excipients

The study of the interactions of excipients with drugs is the essential step in pre-formulation studies. DSC is an analytical method that is frequently used to assess drug-excipient interactions. Any change in the endothermic or exothermic peak and/or enthalpy values indicates a probable interaction. Additives that are expected to be used in the appropriate proportions for the development of polymer micelles of DTX were selected for the study. Differential injection calorimetry (DSC) of the physical mixture of P188, folic acid, and P188-FA was performed using an open-fan DSC Q20, and the results were analyzed using Universal Analysis Software version 4.5A. The interpretation of thermal data isn't always clear; Therefore, Fourier Transforms Infrared Spectroscopy (FTIR) is used to minimize misinterpretation of DSC results. IR spectra of P188, Folic acid, and the physical mixture of P188-FA were recorded on an FTIR spectrophotometer (MAKE) using potassium bromide pellets in the range of 4000–500 cm<sup>-1</sup>.

### 4.3 Synthesis of FA- P188 Conjugate

A scheme for conjugate formation is given in figure 13 and figure 14. Briefly, Folic acid (1.6 g) was dissolved in a mixture of DMAP (0.1g) and DMSO (10ml); Another solution of Poloxamer P188 (0.15g) in dry chloromethane was prepared. Both these solutions were mixed while stirring at low temperatures, followed by a dropwise addition of DCC. A mixture of folic acid and DMAP and DMSO was kept at room temperature for 48 hours to complete the reaction. It was then extracted with a 10% NaHCO<sub>3</sub> solution to remove the unreacted folic acid. The organophases obtained after extraction were refrigerated overnight for crystallization and filtered to remove insoluble substances. This organic solution then precipitated twice using cold diethyl ether. The resulting product was filtered and dried overnight under a vacuum and stored until further use. The generation of FA- P188 was confirmed by proton nuclear magnetic resonance analysis (1H NMR) obtained at 400 MHz.

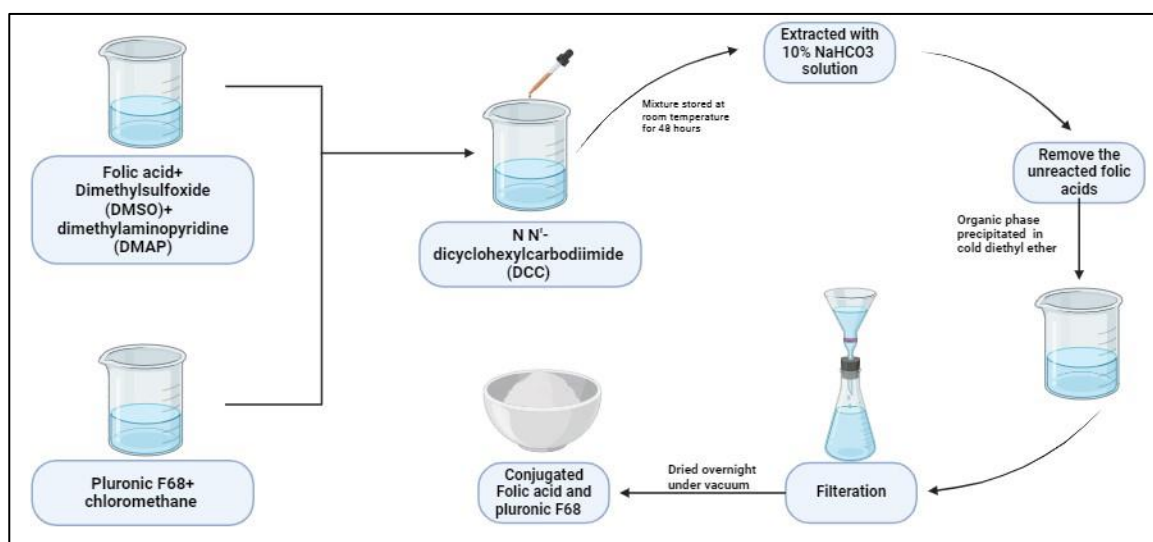


**Figure 13.** Folic acid and Poloxamer P188 were conjugated using DMAP, DCC, and DMSO.

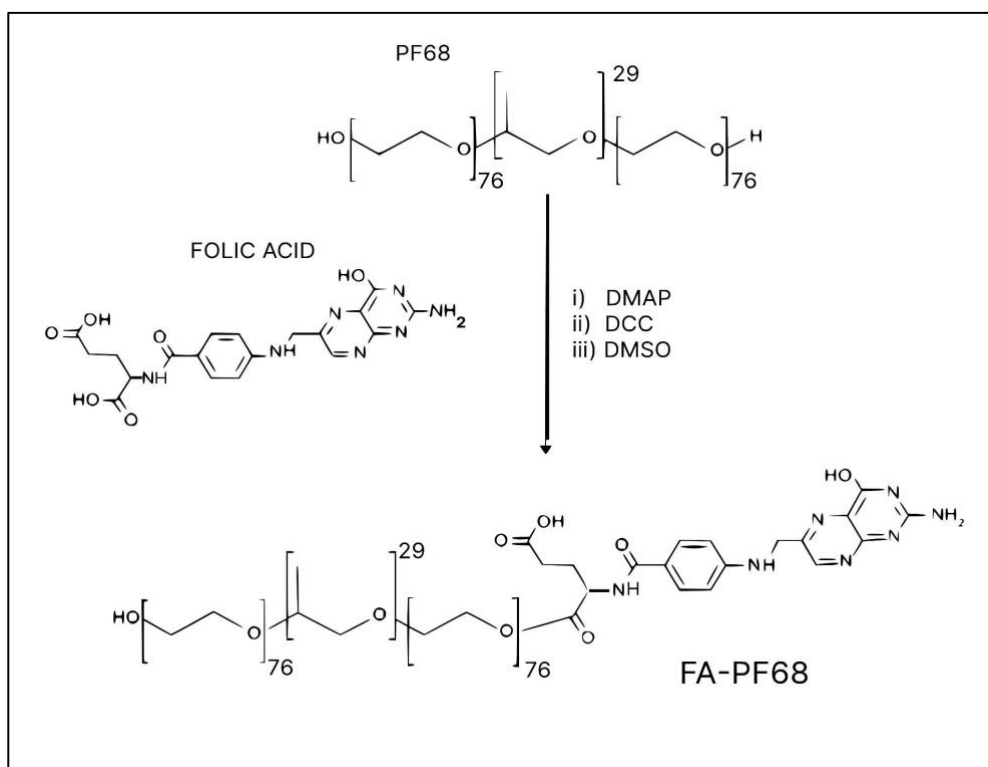


**Figure 14.** Schematic illustration for the synthesis of FA-P188 conjugation; Folic acid and Poloxamer P188 were conjugated by esterification reaction, using DMAP, DCC, and DMSO.

#### 4.4 Preparation of P188-DTX & FA-P188-DTX micelles

P188-DTX & FA-P188-DTX conjugated micelles were prepared by the previously reported thin-film hydration method (THF) with some modification [42]. Briefly, 150 mg of P188 and 5 mg of DTX was dissolved in 3 mL acetonitrile and sonicated for 3 min 10 times. Further the mixture was evaporated at 65°C for 30 minutes using rotary evaporator. A thin film formed on the inner surface of the round-bottomed flask of the rotary evaporator, which was placed in a dryer to remove the solvent. The dried thin films were hydrolyzed in 5 mL of purified water at 40°C and continuous stirring. The solution was then filtered with a 0.44  $\mu$  membrane filter. Similarly, FA-P188-DTX micelles were manufactured by using folate-bound P188 instead of P188 and performing the same process.

#### 4.5 Experimental design, statistical analysis, and optimization

The variables in this study were optimized using a  $3^2$  randomized whole-planing design [43]. This study evaluated two variables at three levels, and all experiments of nine potential combinations were performed. The amount of binding polymer (FA-P188) and drug (DTX) were selected as independent variables. These variables ranged from 3 levels: low (-1), medium (0), and high (+1). Carrier efficiency and particle size were selected as dependent variables (Table 6). Data obtained from all formulations were analyzed with Design-Expert software, and study designs and reaction surface plots were generated. The software was used to generate polynomial models for all response variables, including linear, interactive, cubic, and quadratic terms. The optimal model was selected based on a comparison of a number of statistical parameters provided by the Design-Expert software, including the coefficient of variation (CV), the coefficient of regression ( $R^2$ ), and the adjusted coefficient of regression (adjusted  $R^2$ ). Additionally, analysis of variance (ANOVA) was used to determine the factors had a significant effect on the response regression coefficient. The software was also used to calculate the F test and P values. For a variety of measured

responses, mathematical model equations involving independent variables and their interactions were used to model the effects of the measured responses of various independent variables. For optimization,  $3^2$  planning designs were used. The relationship between the dependent and independent variables was determined using Response surface plots. These plots were used to investigate the influence of various factors on response at specific time points and to predict dependent variable responses in moderate independent variables. Then, using a numerical optimization technique based on the desirability approach and a graphical optimization strategy based on the overlay plot, new formulations with the desired response were generated [44].

**Table 6.**  $3^2$  full factorial design: factors, factor levels and responses.

Factors (Independent variables)	Factor levels used		
	Low (-1)	Medium (0)	High (1)
FA-P188 mg ( $X_1$ )	100	150	200
DTX mg ( $X_2$ )	5	10	15
<b>Responses (dependent variables)</b>			
% EE (%) ( $Y_1$ )			
PS (nm) ( $Y_2$ )			

#### 4.6 Validation of the experimental design

The experimental values of the response were quantitatively compared with the predicted values to validate the selected experimental design, and the relative error (%) was estimated using the following equation:

$$\text{Relative error (\%)} = \frac{\text{Predicted value} - \text{Experimental value}}{\text{Predicted value}} \times 100$$

#### 4.7 Characterization of P188-DTX & FA-P188-DTX Micelles

##### 4.7.1 Critical micelle concentration (CMC) determination

UV spectroscopy was used to determine the CMC of P188 and FA-P188 [45]. The standard solution was prepared by dissolving 0.5 g of iodine and 1.0 g of potassium iodide in 50 mL of deionized water. Different concentrations of polymer solutions between 0.001% and 0.01% were prepared. Depending on the polymer concentration, 30-50  $\mu$ L of standard solution was added to the polymer solution. Prior to measurement, the solutions were incubated at room temperature for 12 hours. UV-Vis spectrophotometers were used to determine the absorbance values of various polymer concentrations. The polymer mass concentration's logarithmic value was plotted for absorbance. The CMC value indicates the concentration of the polymer with a rapid increase in absorbance.

##### 4.7.2 Particle size, polydispersity index, and zeta potential

Particle size and Polydispersity index of P188-DTX and FA-P188-DTX micelles were determined by the dynamic light scattering (DLS) method using Zetasizer® nano (Model: Zen 3600, Malvern Instruments, UK). The zeta potential was measured from the electrophoretic mobility of micelles. To elucidate the existence of P188-DTX and FA-P188-DTX micelles, they were visualized using a scanning electron microscope (SEM) at a magnification up to 20.00 kV and with an accelerating voltage of 100 kV.

##### 4.7.3 Determination of Percent Entrapment Efficiency (%EE)

The entrapment efficiency (EE) of P188-DTX and FA-P188 DTX conjugated micelles was done by the ultracentrifugation method using a Remi cooling centrifuge (Remi Elektrotechnik Ltd., India). The



supernatant containing untrapped drug was removed and analyzed by UV spectrophotometry (at  $\lambda_{max}$  = 230 nm) (Model: SPECTRO 2060 PLUS, Analytical Technologies Ltd., Gujarat, India) against a 30: 70 ratio of methanol: phosphate buffer solution (PBS) (pH 7.4).

The amount of drug entrapped in micelles was determined by an equation given below.

$$\%EE = \frac{\text{Total amount of drug} - \text{untrapped drug}}{\text{Total amount of drug}} \times 100$$

#### 4.7.4 In Vitro Drug Release

The in vitro drug release from P188-DTX and FA-P188-DTX micelles was determined using the dialysis method [46]. Briefly, 2 mL of P188-DTX and FA-P188-DTX micelles were placed in a pre-swelled dialysis pouch (MW 3500 Da) and dialysis was performed in 100 mL of phosphate buffer (pH 7.4) at a frequency of 100 rpm at 0.5 °C at 37 ±. Samples were taken at predetermined time intervals and the dose was refilled with the same amount of fresh buffer. The emitted DTX was analyzed by UV spectroscopy.

#### 4.7.5 Haemolytic toxicity assay

Spectrophotometry-based hemolysis analysis was performed to assess hemo-compatibility [47]. Blood samples were collected from healthy donors in EDTA-treated vials. Red blood cells were centrifuged at 3000 rpm for 5-10 min at 4°C. A red blood cell suspension diluted with normal saline was prepared at a concentration of 5% w/v. Erythrocyte suspension (0.5 mL) was mixed with purified water (considered to cause 100% hemolysis), normal saline (blank) that does not cause hemolysis, DTX solution, and FA-P188-DTX micelle formulation in the concentration range of 50~200 µg/mL. After incubation at 37°C for 1 hour with slow shaking, the mixture was centrifuged at 3000 rpm for 10 min to separate undissolved red blood cells. The supernatant was taken, and diluted with the same amount of PBS (pH 7.4), and absorbance was measured at 540 nm for the normal saline supernatant. The equation given below was used to determine the percentage of haemolysis for each sample:

$$\% \text{ Hemolysis} = \frac{\text{Absorbance of Sample}}{\text{Absorbance of 100\% lysis}} \times 100$$

#### 4.7.6 In Vitro Cytotoxicity Study

MDA-MB-231 cells (human breast adenocarcinoma) were used to evaluate the anticancer activity of the formulation [48]. The in vitro cytotoxicity of FA-P188-DTX micelles and DTX-solution was done for 72 hours using MTT assay. MDA-MB-231 cells were inoculated in 96-well plates at a density of  $10^4$  cells per well ×  $10^4$  cells per well for 24 hours. The micelles loaded with DTX and DTX solutions were diluted to different concentrations (2, 8, 12, 20, 40 µg/mL) to prepare the suspension. The medium was replaced with 200 µL of sample solution and incubated in a CO2 incubator at 37°C for 72 hours. After incubation, the medium was replaced with fresh medium and 50 µL of MTT Reagent (1 mg/mL in PBS) was added to each well. After the plates were incubated again at 37°C for 3 hours, the medium was removed and the intracellular formazan was dissolved in 160 µL DMSO. Absorbance was measured at 570 nm using SpectraMaxM2 with SoftMax Pro (Molecular Devices Corporation Sunnyvale, CA, USA). Cells treated with medium were used as a control group, and cell survival percentages were calculated based on the absorbance of cells exposed to the control group.

$$\text{cell viability}(\%) = \frac{\text{Absorbance of cells exposed to the sample}}{\text{Absorbance of untreated cells}} \times 100\%$$

#### 4.7.7 Stability study

Accelerated stability test of FA-P188-DTX micelles was performed for 3 months under the following conditions: 40±2°C temperature and 75±5% RH (RH) under the following conditions: This trial is intended to determine the stability potential of the drug in its current formulation.

**Acknowledgements:** The authors are grateful to the Department of Pharmaceutics, Smt. Kishoritai Bhoyar College of Pharmacy,

Kamptee, Nagpur for providing the lab and equipment facilities.

**Author contributions:** All authors contributed to the study conception and design. Material, preparation, data collection, and analysis were performed by Amol Tatode and Divya Zambre. The first draft of the manuscript was written by Mohammad Qutub and Tanvi Premchandani, then modified and edited by Prashant Pande and Milind Umekar. Amol Tatode and all authors commented on previous versions of the manuscript. All authors read and approved the final manuscript.

**Conflict of interest statement:** The authors declared no conflict of interest.

## REFERENCES

- [1] Yao Q, Choi JH, Dai Z, Wang J, Kim D, Tang X, Zhu L. Improving tumor specificity and anticancer activity of dasatinib by dual-targeted polymeric micelles. *ACS Appl Mater Interfaces*. 2017;9(42):36642-36654. <http://dx.doi.org/10.1021/acsami.7b12233>
- [2] Wang Z, Chen C, Liu R, Fan A, Kong D, Zhao Y. Two birds with one stone: dendrimer surface engineering enables tunable periphery hydrophobicity and rapid endosomal escape. *Chem Commun*. 2014;50(90):14025-14028. <http://dx.doi.org/10.1039/C4CC06621A>
- [3] Zhang J, Yang PL, Gray NS. Targeting cancer with small molecule kinase inhibitors. *Nat Rev Cancer*. 2009;9(1):28-39. <http://dx.doi.org/10.1038/nrc2559>
- [4] Fathi Karkan S, Davaran S, Akbarzadeh A. Cisplatin-loaded superparamagnetic nanoparticles modified with PCL-PEG copolymers as a treatment of A549 lung cancer cells. *Nanomed Res J*. 2019;4(4):209-219. <http://dx.doi.org/10.22034/nmrj.2019.04.002>
- [5] Chen Y, Chen H, Shi J. Inorganic nanoparticle-based drug codelivery nanosystems to overcome the multidrug resistance of cancer cells. *Mol Pharm*. 2014;11(8):2495-2510. <http://dx.doi.org/10.1021/mp400596v>
- [6] Pirmohamed T, Dowding JM, Singh S, Wasserman B, Heckert E, Karakoti AS, King JES, Seal S, Self WT. Nanoceria exhibit redox state-dependent catalase mimetic activity. *Chem Commun*. 2010;46(16):2736. <http://dx.doi.org/10.1039/b922024k>
- [7] Korsvik C, Patil S, Seal S, Self WT. Superoxide dismutase mimetic properties exhibited by vacancy engineered ceria nanoparticles. *Chem Commun*. 2007;10:1056. <http://dx.doi.org/10.1039/b615134e>
- [8] Fares AR, ElMeshad AN, Kassem MAA. Enhancement of dissolution and oral bioavailability of lacidipine via pluronic P123/F127 mixed polymeric micelles: formulation, optimization using central composite design and in vivo bioavailability study. *Drug Deliv*. 2018;25(1):132-142. <http://dx.doi.org/10.1080/10717544.2017.1419512>
- [9] Zhang CY, Peng S, Zhao B, Luo W, Zhang L. Polymeric micelles self-assembled from amphiphilic polymers with twin disulfides used as siRNA carriers to enhance the transfection. *Mater Sci Eng C*. 2017;78:546-552. <http://dx.doi.org/10.1016/j.msec.2017.04.039>
- [10] Farasati Far B, Maleki-baladi R, Fathi-karkan S, Babaei M, Sargazi S. Biomedical applications of cerium vanadate nanoparticles: A review. *J Mater Chem B*. 2024;12(3):609-636. <http://dx.doi.org/10.1039/D3TB01786A>
- [11] Ding J, Chen L, Xiao C, Chen L, Zhuang X, Chen X. Noncovalent interaction-assisted polymeric micelles for controlled drug delivery. *Chem Commun*. 2014;50(77):11274-11290. <http://dx.doi.org/10.1039/C4CC03153A>
- [12] Zhang H, Wang K, Zhang P, He W, Song A, Luan Y. Redox-sensitive micelles assembled from amphiphilic mPEG-PCL-SS-DTX conjugates for the delivery of docetaxel. *Colloids Surf B Biointerfaces*. 2016;142:89-97. <http://dx.doi.org/10.1016/j.colsurfb.2016.02.045>
- [13] Biswas S, Kumari P, Lakhani PM, Ghosh B. Recent advances in polymeric micelles for anti-cancer drug delivery. *Eur J Pharm Sci*. 2016;83:184-202. <http://dx.doi.org/10.1016/j.ejps.2015.12.031>
- [14] Cagel M, Tesan FC, Bernabeu E, Salgueiro MJ, Zubillaga MB, Moretton MA, Chiappetta DA. Polymeric mixed micelles as nanomedicines: Achievements and perspectives. *Eur J Pharm Biopharm*. 2017;113:211-228. <http://dx.doi.org/10.1016/j.ejpb.2016.12.019>
- [15] Amjad MW, Kesharwani P, Mohd Amin MCI, Iyer AK. Recent advances in the design, development, and targeting mechanisms of polymeric micelles for delivery of siRNA in cancer therapy. *Prog Polym Sci*. 2017;64:154-181. <http://dx.doi.org/10.1016/j.progpolymsci.2016.09.008>
- [16] Martín-Sabroso C, Torres-Suárez AI, Alonso-González M, Fernández-Carballido A, Fraguas-Sánchez AI. Active Targeted Nanoformulations via Folate Receptors: State of the Art and Future Perspectives. *Pharmaceutics*. 2021;14(1):14. <http://dx.doi.org/10.3390/pharmaceutics14010014>
- [17] Wu Q, Zheng H, Gu J, Cheng Y, Qiao B, Wang J, Xiong L, Sun S, Wu Z, Bao A, Tong Y. Detection of folate receptor-positive circulating tumor cells as a biomarker for diagnosis, prognostication, and

- therapeutic monitoring in breast cancer. *J Clin Lab Anal.* 2022;36(1): e24180. <http://dx.doi.org/10.1002/jcla.24180>
- [18] Chen Q, Zheng J, Yuan X, Wang J, Zhang L. Folic acid grafted and tertiary amino based pH-responsive pentablock polymeric micelles for targeting anticancer drug delivery. *Mater Sci Eng C.* 2018;82:1-9. <http://dx.doi.org/10.1016/j.msec.2017.08.026>
- [19] Chen Y, Tezcan O, Li D, Beztsinna N, Lou B, Etrych T, Ulbrich K, Metselaar JM, Lammers T, Hennink WE. Overcoming multidrug resistance using folate receptor-targeted and pH-responsive polymeric nanogels containing covalently entrapped doxorubicin. *Nanoscale.* 2017;9(29):10404-10419. <http://dx.doi.org/10.1039/C7NR03592F>
- [20] Javad Javid-Naderi M, Valizadeh N, Banimohamad-Shotorbani B, Shahgolzari M, Shayegh F, Maleki-baladi R, Sargazi S, Fathi-karkan S. Exploring the biomedical potential of iron vanadate Nanoparticles: A comprehensive review. *Inorg Chem Commun.* 2023;157:111423. <http://dx.doi.org/10.1016/j.inoche.2023.111423>
- [21] Zhang X, Liang N, Gong X, Kawashima Y, Cui F, Sun S. Tumor-targeting micelles based on folic acid and  $\alpha$ -tocopherol succinate conjugated hyaluronic acid for paclitaxel delivery. *Colloids Surf B Biointerfaces.* 2019;177:11-18. <http://dx.doi.org/10.1016/j.colsurfb.2019.01.044>
- [22] Dai Y, Cai X, Bi X, Liu C, Yue N, Zhu Y, Zhou J, Fu M, Huang W, Qian H. Synthesis and anti-cancer evaluation of folic acid-peptide- paclitaxel conjugates for addressing drug resistance. *Eur J Med Chem.* 2019;171:104-115. <http://dx.doi.org/10.1016/j.ejmech.2019.03.031>
- [23] Bodratti AM, Alexandridis P. Amphiphilic block copolymers in drug delivery: advances in formulation structure and performance. *Expert Opin Drug Deliv.* 2018;15(11):1085-1104. <http://dx.doi.org/10.1080/17425247.2018.1529756>
- [24] de Castro KC, Coco JC, dos Santos EM, Ataíde JA, Martinez RM, do Nascimento MHM, Prata J, da Fonte PRML, Severino P, Mazzola PG, Baby AR, Souto EB, de Araujo DR, Lopes AM. Pluronic® triblock copolymer-based nanoformulations for cancer therapy: A 10-year overview. *J Control Release.* 2023;353:802-822. <http://dx.doi.org/10.1016/j.jconrel.2022.12.017>
- [25] Mustafa G, Hassan D, Zeeshan M, Ruiz-Pulido G, Ebrahimi N, Mobashar A, Pourmadadi M, Rahdar A, Sargazi S, Fathi-karkan S, Medina DI, Díez-Pascual AM. Advances in nanotechnology versus stem cell therapy for the theranostics of Huntington's disease. *J Drug Deliv Sci Technol.* 2023;87:104774. <https://doi.org/10.1016/j.jddst.2023.104774>
- [26] Batrakova E V., Kabanov A V. Pluronic block copolymers: Evolution of drug delivery concept from inert nanocarriers to biological response modifiers. *J Control Release.* 2008;130(2):98-106. <http://dx.doi.org/10.1016/j.jconrel.2008.04.013>
- [27] Raval A, Parmar A, Raval A, Bahadur P. Preparation and optimization of media using Pluronic® micelles for solubilization of sirolimus and release from the drug eluting stents. *Colloids Surf B Biointerfaces.* 2012;93:180-187. <http://dx.doi.org/10.1016/j.colsurfb.2011.12.034>
- [28] Guzmán Rodríguez A, Sablón Carrazana M, Rodríguez Tanty C, Malessy MJA, Fuentes G, Cruz LJ. Smart polymeric micelles for anticancer hydrophobic drugs. *Cancers (Basel).* 2022;15(1):4. <http://dx.doi.org/10.3390/cancers15010004>
- [29] Zhang W, Shi Y, Chen Y, Hao J, Sha X, Fang X. The potential of Pluronic polymeric micelles encapsulated with paclitaxel for the treatment of melanoma using subcutaneous and pulmonary metastatic mice models. *Biomaterials.* 2011;32(25):5934-5944. <http://dx.doi.org/10.1016/j.biomaterials.2011.04.075>
- [30] Anirudhan TS, Varghese S, Manjusha V. Hyaluronic acid coated Pluronic F127/Pluronic P123 mixed micelle for targeted delivery of Paclitaxel and Curcumin. *Int J Biol Macromol.* 2021;192:950-957. <http://dx.doi.org/10.1016/j.ijbiomac.2021.10.061>
- [31] Saghati S, Rahbarghazi R, Fathi Karkan S, Nazifkardar S, Khoshfetrat AB, Tayefi Nasrabadi H. Shape memory polymers in osteochondral tissue engineering. *J Res Clin Med.* 2022;10(1):30. <http://dx.doi.org/10.34172/jrcm.2022.030>
- [32] Banimohamad-Shotorbani B, Karkan SF, Rahbarghazi R, Mehdipour A, Jarolmasjed S, Saghati S, Shafaei H. . Application of mesenchymal stem cell sheet for regeneration of craniomaxillofacial bone defects. *Stem Cell Res Ther.* 2023;14(1):68. <http://dx.doi.org/10.1186/s13287-023-03309-4>
- [33] Balasubramaniam A, Panpalia GM. Drug Adjuvant Interaction Study Using DSC Supported by Isothermal Method. *Drug Dev Ind Pharm.* 2001;27(5):475-480. <http://dx.doi.org/10.1081/DDC-100104324>

- [34] Fathi-Karkan S, Heidarzadeh M, Narmi MT, Mardi N, Amini H, Saghati S, Abrbekoh FN, Saghebasl S, Rahbarghazi R, Khoshfetrat AB. Exosome-loaded microneedle patches: Promising factor delivery route. *Int J Biol Macromol*. 2023;243:125232. <http://dx.doi.org/10.1016/j.ijbiomac.2023.125232>
- [35] Pourmadadi M, Ostovar S, Ruiz-Pulido G, Hassan D, Souiri M, Manicum A-LE, Behzadmehr R, Fathi-karkan S, Rahdar A, Medina DI, Pandey S. Novel epirubicin-loaded nanoformulations: Advancements in polymeric nanocarriers for efficient targeted cellular and subcellular anticancer drug delivery. *Inorg Chem Commun*. 2023;155:110999. <http://dx.doi.org/10.1016/j.inoche.2023.110999>
- [36] Roostae M, Derakhshani A, Mirhosseini H, Banaee Mofakham E, Fathi-Karkan S, Mirinejad S, Sargazi S, Barani M. Composition, preparation methods, and applications of nanoniosomes as codelivery systems: a review of emerging therapies with emphasis on cancer. *Nanoscale*. 2024;16(6):2713-2746. <http://dx.doi.org/10.1039/D3NR03495J>
- [37] Fathi-karkan S, Zeeshan M, Qindeel M, Eshaghi Malekshah R, Rahdar A, Ferreira LFR. NPs loaded with zoledronic acid as an advanced tool for cancer therapy. *J Drug Deliv Sci Technol*. 2023;87:104805. <http://dx.doi.org/10.1016/j.jddst.2023.104805>
- [38] Bakhshi S, Shoari A, Alibolandi P, Ganji M, Ghazy E, Rahdar A, Fathi-karkan S, Pandey S. Emerging innovations in vincristine-encapsulated nanoparticles: Pioneering a new era in oncological therapeutics. *J Drug Deliv Sci Technol*. 2024;91:105270. <http://dx.doi.org/10.1016/j.jddst.2023.105270>
- [39] Pourmadadi M, Gerami SE, Ajalli N, Yazdian F, Rahdar A, Fathi-karkan S, Aboudzadeh MA. Novel pH-responsive hybrid hydrogels for controlled delivery of curcumin: Overcoming conventional constraints and enhancing cytotoxicity in MCF-7 cells. *Hybrid Adv*. 2024;6:100210. <http://dx.doi.org/10.1016/j.hybadv.2024.100210>
- [40] Fatima I, Zeinalilathori S, Qindeel M, Kharaba Z, Sahebzade MS, Rahdar A, Zeinali S, Fathi-karkan S, Khan A, Ghazy E, Pandey S. Advances in targeted nano-delivery of bevacizumab using nanoparticles: Current insights, innovations, and future perspectives. *J Drug Deliv Sci Technol*. 2024;98:105850. <http://dx.doi.org/10.1016/j.jddst.2024.105850>
- [41] Davodabadi F, Mirinejad S, Malik S, Dhasmana A, Ulucan-Karnak F, Sargazi S, Sargazi S, Fathi-Karkan S, Rahdar A. Nanotherapeutic approaches for delivery of long non-coding RNAs: an updated review with emphasis on cancer. *Nanoscale*. 2024;16(8):3881-3914. <http://dx.doi.org/10.1039/D3NR05656B>
- [42] Liu Z, Liu D, Wang L, Zhang J, Zhang N. Docetaxel-Loaded Pluronic P123 Polymeric Micelles: in Vitro and in Vivo Evaluation. *Int J Mol Sci*. 2011;12(3):1684-1696. <http://dx.doi.org/10.3390/ijms12031684>
- [43] Bolton S, Bon C. *Pharmaceutical Statistics: Practical and Clinical Applications, Revised and Expanded*, fourth ed. CRC Press (2003). <http://dx.doi.org/10.1201/9780203912799>
- [44] Acharya S, Patra S, Pani NR. Optimization of HPMC and carbopol concentrations in non-effervescent floating tablet through factorial design. *Carbohydr Polym*. 2014;102:360-368. <http://dx.doi.org/10.1016/j.carbpol.2013.11.060>
- [45] Gaisford S, Beezer AE, Mitchell JC, Loh W, Finnie JK, Williams SJ. Diode-array UV spectrometric evidence for a concentration dependent phase transition in dilute aqueous solutions of pluronic F87 (poloxamer 237). *J Chem Soc Chem Commun*. 1995;18:1843. <http://dx.doi.org/10.1039/c39950001843>
- [46] Cho YW, Lee J, Lee SC, Huh KM, Park K. Hydrotropic agents for study of in vitro paclitaxel release from polymeric micelles. *J Control Release*. 2004;97(2):249-257. <http://dx.doi.org/10.1016/j.jconrel.2004.03.013>
- [47] Evans BC, Nelson CE, Yu SS, Beavers KR, Kim AJ, Li H, Nelson HM, Giorgio TD, Duvall CL. Ex vivo red blood cell hemolysis assay for the evaluation of pH-responsive endosomolytic agents for cytosolic delivery of biomacromolecular drugs. *J Vis Exp*. 2013;73:e50166. <http://dx.doi.org/10.3791/50166>
- [48] Razak NA, Abu N, Ho WY, Zamberi NR, Tan SW, Alitheen NB, Long K, Yeap SK. Cytotoxicity of eupatorin in MCF-7 and MDA-MB-231 human breast cancer cells via cell cycle arrest, anti-angiogenesis and induction of apoptosis. *Sci Rep*. 2019;9(1):1514. <http://dx.doi.org/10.1038/s41598-018-37796-w>